INFLUENCE OF DE-VEGETATION ON LAND SURFACE TEMPERATURE: A CASE STUDY OF BARDEZ TALUKA, GOA-INDIA

Article · January 2022

DOI: 10.31032/IJBPAS/2022/11.1.1076

2 authors, including:

F M Nadaf
DPM's Shree Mallikarjun & Shri. Chetan Manju Desai College, Canacona Goa India
38 PUBLICATIONS **30** CITATIONS

SEE PROFILE

IJBPAS, January, Special Issue, 2022, 11(1): 614-627

ISSN: 2277–4998

International Journal of Biology, Pharmacy and Allied Sciences (IJBPAS)

'A Bridge Between Laboratory and Reader'

www.ijbpas.com

INFLUENCE OF DE-VEGETATION ON LAND SURFACE TEMPERATURE: A CASE STUDY OF BARDEZ TALUKA, GOA-INDIA

VENKATESH G. PRABHU GAONKAR[1*], F.M. NADAF[2]

1: Assistant Professor in Geoinformatics, S. P. Chowgule College, Margao Goa, India

2: Professor of Geography, DPM's Shree Mallikarjun and Shri Chetan Manju Desai College, Canacona-Goa, India

[*]**Corresponding Author: Dr. Venkatesh G. Prabhu Gaonkar**

Received 10th June 2021; Revised 11th July 2021; Accepted 20th Aug. 2021; Available online 15th Jan. 2022

https://doi.org/10.31032/IJBPAS/2022/11.1.1076

ABSTRACT

The Earth's climate has warmed by around 0.6 degrees Celsius over the last century, with two big phases of warming between 1910 and 1945, and from 1976 onwards. Land Surface Temperature is an important parameter in land surface processes because it serves as an indicator of climate change. Vegetation may be recognized from most other materials using remote sensing data due to its noticeable absorption in the red and blue regions of the visible spectrum, increased green reflectance, and, most importantly, it's very strong reflectance in the near-IR.

For the study area satellite data of the years, 1991 and 2021 was obtained. Different algorithms were employed for the calculations of spectral radiance, brightness temperature, NDVI, the proportion of vegetation, land emissivity, and by considering the output of brightness temperature and land emissivity LST was generated.

As a result, the highest NDVI was 0.72 and the lowest was -0.56 in the year 1991, in the year 2021 NDVI highest value was 0.50 and the lowest value was -0.10. The highest temperature observed in 1991 was 38.1507 °C, while the lowest being 20.6068 °C whereas, for the year 2021, the maximum temperature observed is 40.5029 °C and the minimum is 27.3012 °C. A shift of 2.35 °C at the higher end and 6.69 °C at the lower end can be seen in land surface temperature. This can be due to de-

vegetation over time as a result of the increase in tourism, commercialization, urbanization, and industrialization.

Keywords: De-vegetation, NDVI, LST, Urbanization, and Commercialization

INTRODUCTION

Variation in Land surface temperature is a paramount indicator of environmental change [1], [2]. Land surface and atmosphere can be detected effectively through the assessment of LST [1]. For investigations of environmental change, Landsat 5 TM and Landsat 8 OLI thermal infrared data with 120 and 100 m spatial resolutions, respectively, were used [3], [4].

To retrieve LST from Landsat data, different m ethods have been developed, along with the sta ndard algorithm [3], [5].

For the given study, temporal data from 1991 and 2021 were analyzed. Landsat TM-5 gives a mono-band for the thermal infrared wavelength of window 10.40 – 12.50 mm. For its contemporary period, it has an advantage over other sensors. On the other hand Landsat-8 (OLI-TIRS) is equipped with two windows of thermal infrared bands [6]. This study also focuses on regional microscopic aspects of change in land surface temperature which is induced by a human intervention that directly results in heat stress in urban settlements [7]. The current study area has an intensive flux of tourists, to cater the interest of visitors rapid change in land-cover is inevitable. In technical terms, low NDVI values surfaces have higher reflectance and brightness values [8], [9].

De-vegetation results in a low NDVI value. NDVI is a widely used technique for assessing crop health. Different places in a field may require different quantities of nitrogen to attain good yields due to geographic heterogeneity in soil qualities [10], [11]. Based on the unique reflectance patterns of vegetation cover, the vegetation index allows to delineate the distribution of vegetation and soil [10]. Vegetation differs from most other materials due to its notable absorption in the red and blue segments of the visible spectrum, higher green reflectance, and especially strong reflectance in the near-IR [10], [12]. It is a significant vegetation index that is commonly used in global environmental and climate change studies.

Area of Investigation

The present study area is Bardez: global destinations for beach tourism, which is a prominent taluka in North Goa. The study area comprises twelve villages. It is bounded by River Chapora in the North, River Mandovi to its South, River Mapusa to the East, and the Arabian Sea on the west.

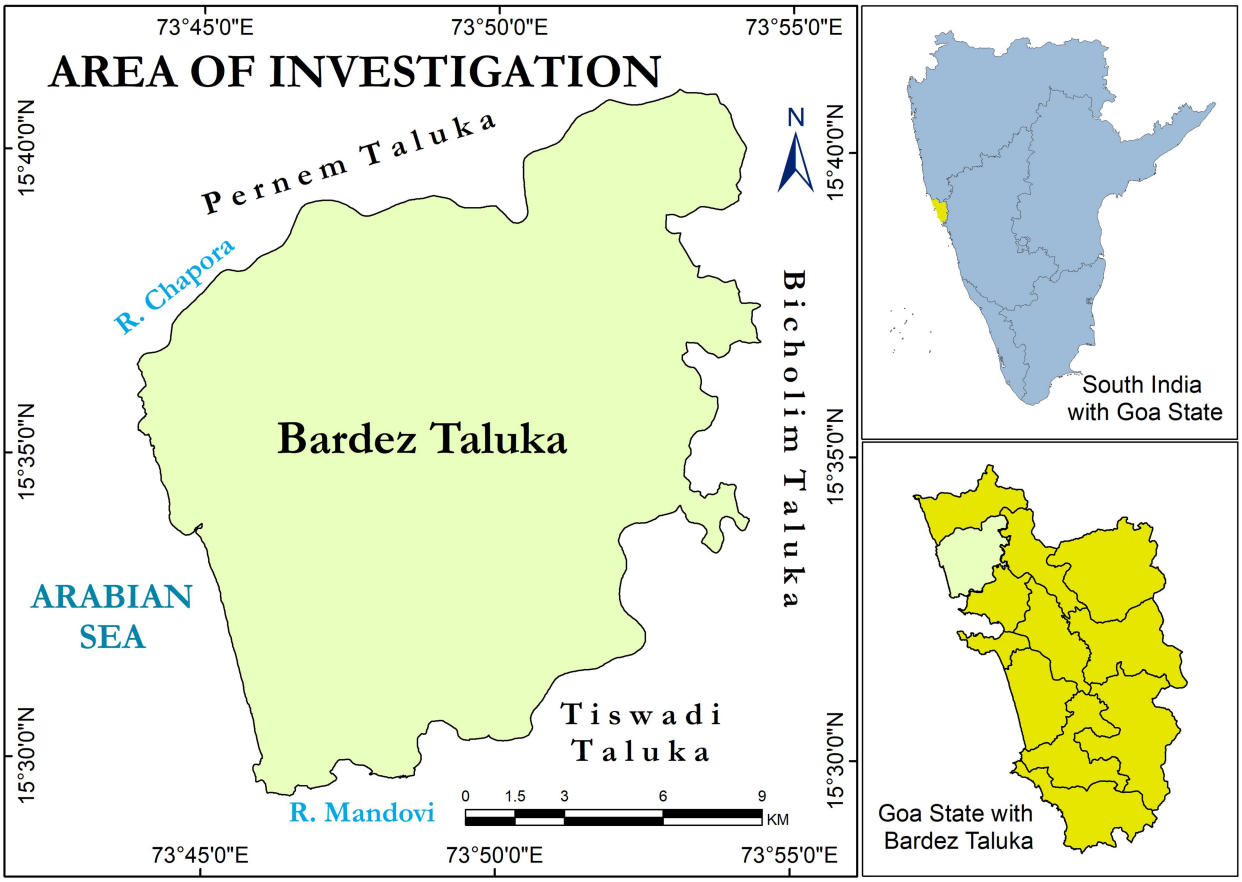

Fig. 1: Area of Investigation

Source: Researcher

Database and Methodology

For the current study, both primary and secondary data were used for analysis. Primary data were obtained from field observations and ground-truthing. Secondary data was obtained from satellite images. Images of Landsat TM-5 and OLI_TIRS-8 were collected from https://glovis.usgs.gov. With 30 meters spatial resolution with 7 and 11 bands respectively. These Landsat images were acquired on 01-02-1991 and 01-02-2021

Satellite images of the years 1991 and 2021 were taken for study purposes. Shapefile were gathered from DIVA-GIS. Later Shapefile was overlayed on satellite images and raster data was extracted. For the given analysis, unique tools were employed. Map algebra which is an implicate part of the calculations required for the determination of LST is an extension of the Spatial analyst tool ArcMap 10.7.1.

Two sets of calculations were performed. Amongst those first results in a determination at sensor temperature. Secondary calculation introduces an effective method to rectify the emissivity values

required for different land surface features.

Top of Atmospheric Radiance:

Calculations for atmospheric spectral radiance using Landsat TM 5:

$$L_{\Delta} = \left(\frac{L_{Max\Delta} - L_{Min\Delta}}{Q_{cal(max)} - Q_{cal(min)}}\right) \times \left(Q_{cal} - Q_{cal(min)}\right) + L_{min\Delta}$$

The meaning of given symbols can be referred from [13]

Calculations for atmospheric spectral radiance using Landsat OLI-TIRS 8:

Spectral radiance determined from Landsat OLI is different from Landsat Thematic Mapper, as Landsat OLI 8 processes 16 bit unsigned data while Landsat TM 5 gives us unsigned 8-bit data. This inherent difference between sensor responses leads us to opt for different methods.

The following formula is obtained from Landsat 8 user handbook provided by the USGS portal

$$L_{\Delta} \;\; = \; M_L \times Q_{cal} + A_l$$

The symbols have their usual meaning those can be referred from[14]

Brightness temperature:

$$BT = \frac{K_2}{\ln(\frac{K_1}{L_{\Delta}}+1)} \text{ [14]}$$

Where,

K1 and K2 are bands specific thermal constants. These values are given in the metadata of raster images. Brightness temperature is at the top of the atmospheric temperature detected by the sensor.

The temperature obtained from the above calculation is in units of Kelvin. It can be converted to degree Celcius by using the following equation:

$$BT(c) = \frac{K_2}{\ln\left(\frac{K_1}{L_{\Delta}}+1\right)} - 273.15 \quad \text{[15], [16]}$$

Normalized Difference Vegetation Index (NDVI)

Vegetation conditions are compared with LST. NDVI gives us information about the presence of vegetation. [15], [17]

$$NDVI = \frac{NIR - Red}{NIR + Red}$$

Table 1: Band combination of Landsat 5 & Landsat 8

Bands	Landsat 5	Landsat 8
Red	3	4
NIR	4	5

The value of NDVI lies between +1 to -1. For NDVI less than 0.2 surface features are considered as bare soil [18]. 0.2-0.5 surface features covered with vegetation and values >0.5 are densely vegetated [19].

The proportion of Vegetation

$$P_v = \left[\frac{NDVI - NDVI_S}{NDVI_v - NDVI_S}\right]^2 \text{[20]}$$

Where,

$NDVI_s$ = 0.2

$NDVI_V$ =0.5

These values are assumed in global conditions [15], [21]

Land Surface Emissivity Estimation

Values of land surface emissivity are employed for the determination of LST. Different land features have different thermal properties [22]. Therefore emissivity values also vary. Emissivity registered for bare soil is 0.970, for vegetation EV is $\xi_6 = 0.986 + 0.004P_v$

Land surfaceemissivity for dense vegetation cover is 0.99. [20]

Land Surface Temperature

Emissivity rectified land surface temperature is computed as:

$$LST = \frac{BT}{1+\left[\left(\frac{\lambda \times BT}{\rho}\right) \times ln\xi\right]}$$ [15], [23]

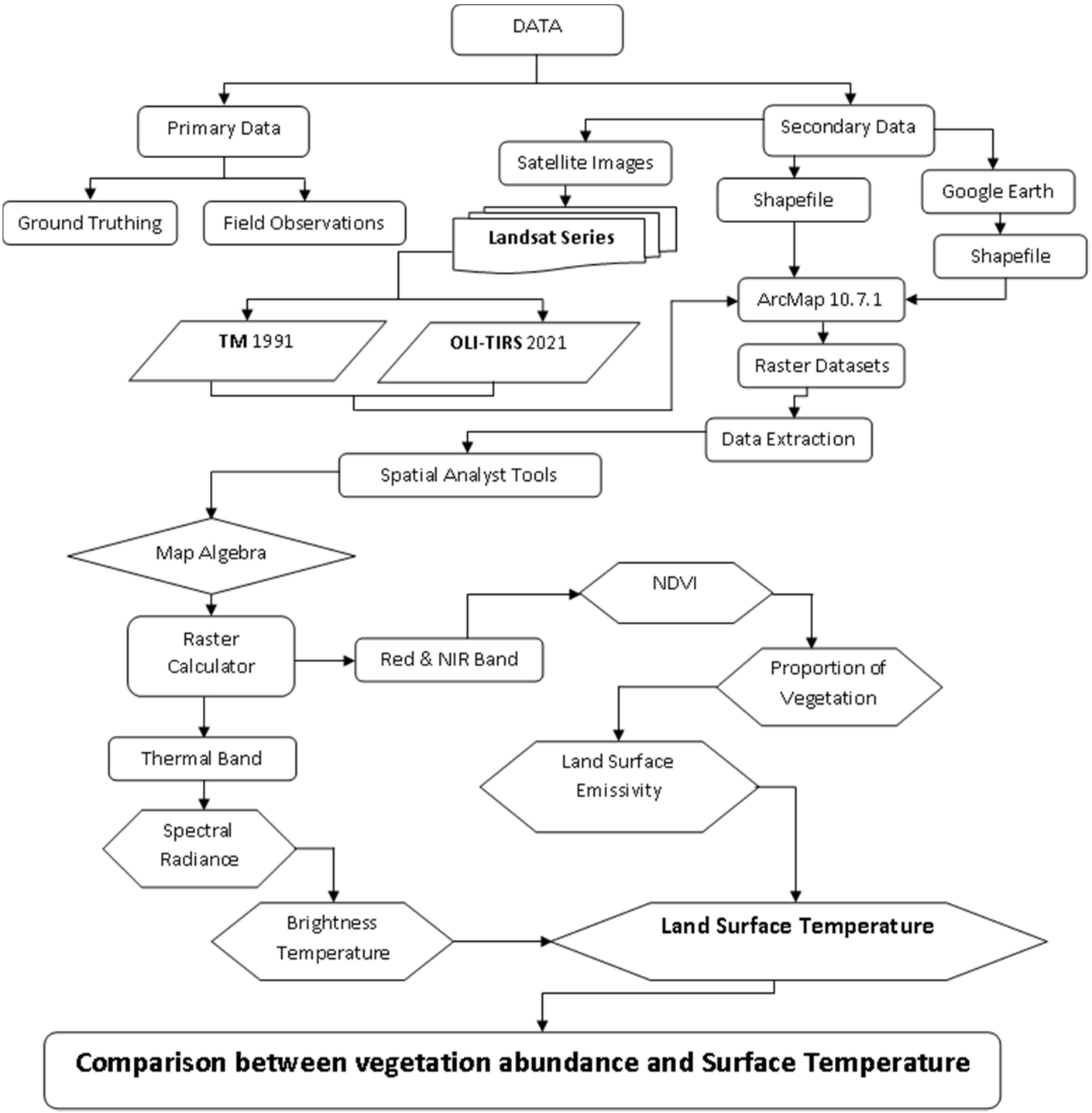

Fig. 2: Methodology chart
Source: Researcher

RESULTS AND DISCUSSION

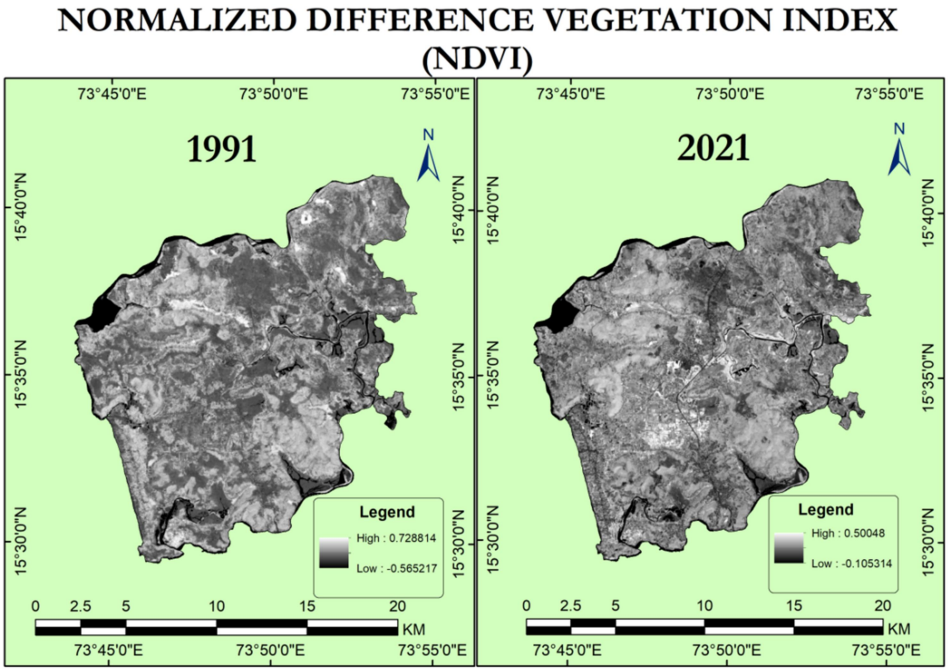

Fig: 3(a) **Fig: 3(b)**

Fig. 3: Comparison of Normalized Difference Vegetation Index (1991 & 2021), Fig: 3(a) NDVI highest: 0.72 and lowest: -0.56, Fig: 3(b) highest: 0.50 and lowest: -0.10

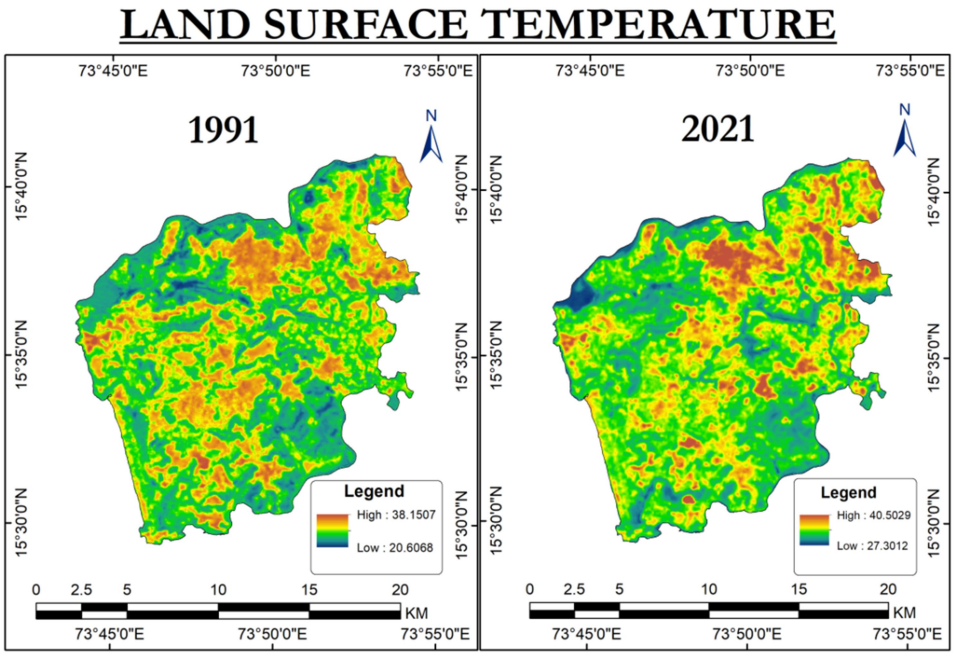

Fig: 4(a) **Fig: 4(b)**

Fig. 4: Comparison of Land Surface Temperature (1991 & 2021),

Fig: 4(a) LST highest: 38.15 and lowest: 20.60, Fig: 4(b) highest: 40.50 and lowest: 27.30

COMPARISION BETWEEN NDVI & LST OF 1991

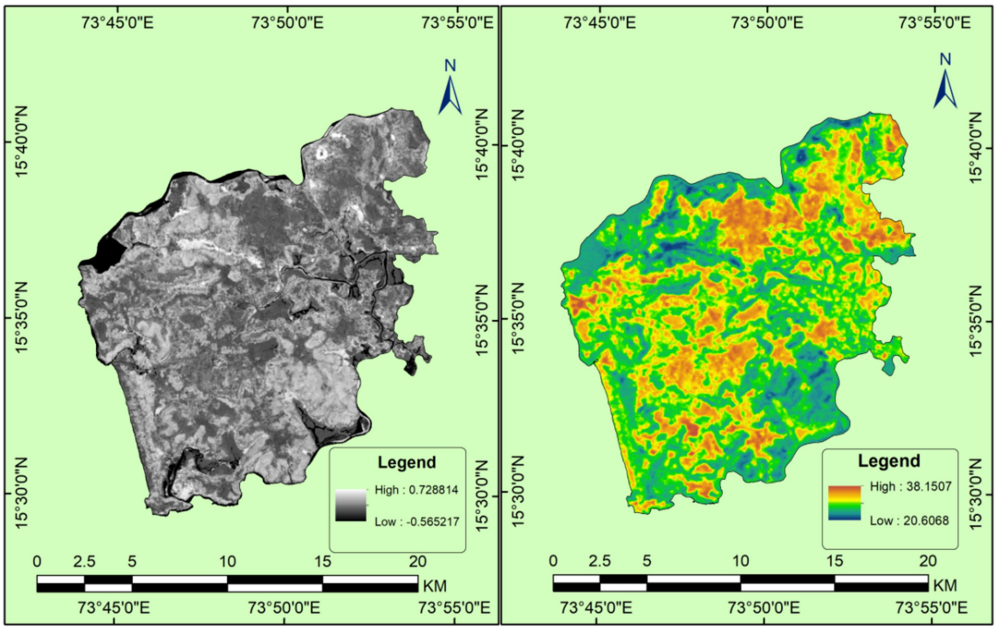

Fig: 5(a) **Fig: 5(b)**

COMPARISION BETWEEN NDVI & LST OF 2021

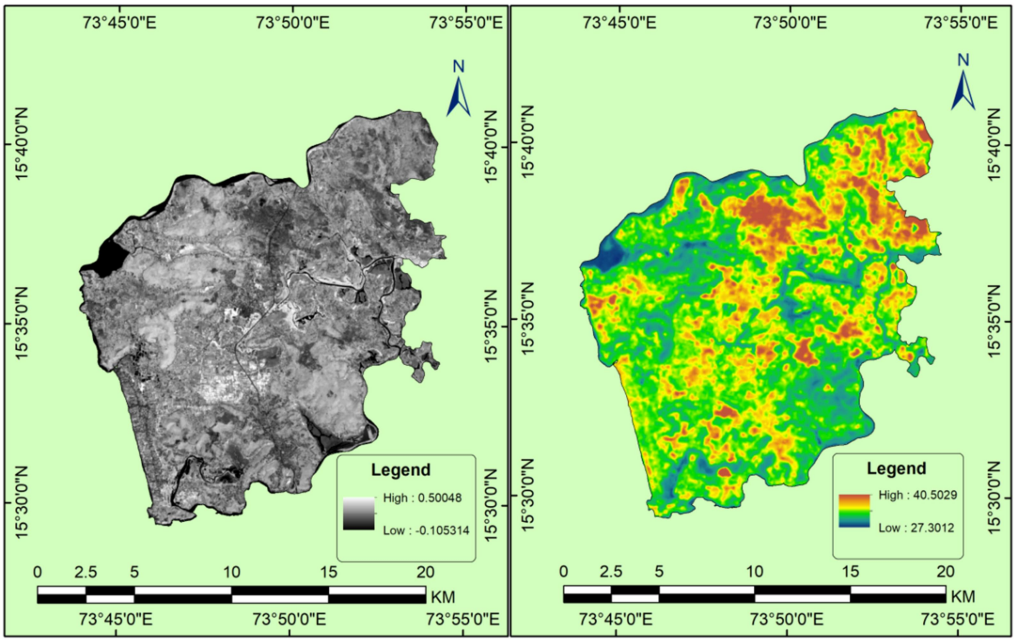

Fig: 6(a) **Fig: 6(b)**

Figure 5 and Figure 6 compares NDVI & LST 1991 and NDVI & LST 2021.

Source: Researcher

Following **figure 7 & table 2** (sample 1), **figure 8 & table 3** (sample 2)**, figure 9 & table 4** (sample 3) **and figure 10 & table 5** (sample 4) compares between NDVI & LST 1991-2021**.**

Source: Researcher

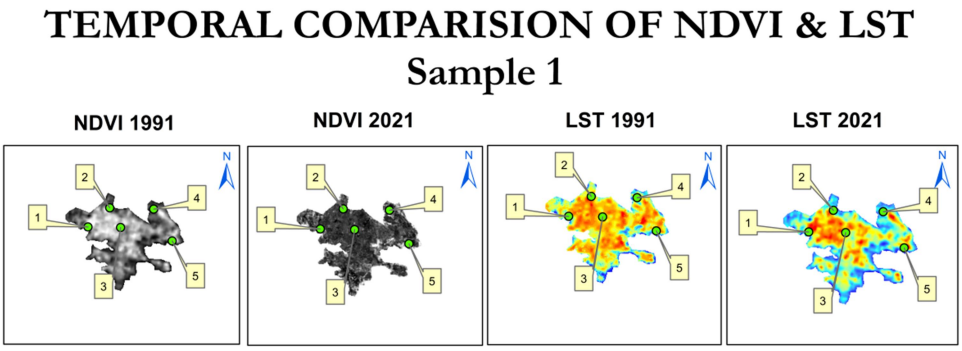

Sr.No.	Longitude	Latittude	NDVI_1991	LST_1991	NDVI_2021	LST_2021
1	73°48'38.704"E	15°37'59.786"N	0.2307	32.9241	0.2124	36.0651
2	73°49'13.294"E	15°38'29.506"N	0.119	34.5781	0.1056	36.3301
3	73°49'30.798"E	15°37'59.115"N	0.1555	33.367	0.1277	35.5818
4	73°50'23.525"E	15°38'27.987"N	0.1494	32.961	0.1294	35.3822
5	73°50'53.386"E	15°37'38.768"N	0.2105	30.9131	0.1639	35.2322

Figure 7 & table 2

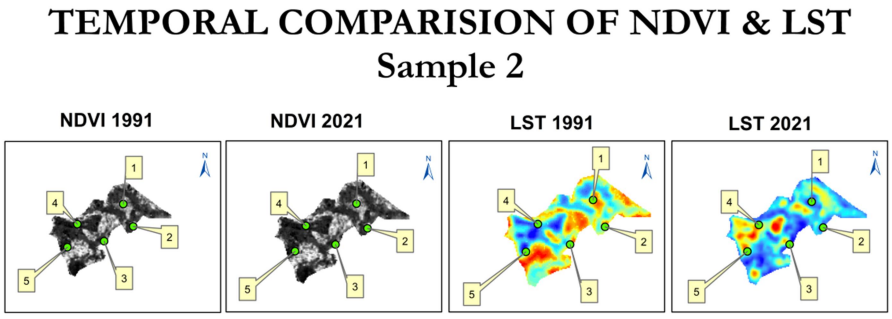

Sr.No.	Longitude	Latittude	NDVI_1991	LST_1991	NDVI_2021	LST_2021
1	73°45'24.114"E	15°35'55.825"N	0.2957	28.4265	0.225	31.5031
2	73°45'35.417"E	15°35'31.507"N	0.3975	28.3273	0.2687	31.5794
3	73°45'2.911"E	15°35'15.343"N	0.2222	28.8679	0.1843	31.7688
4	73°44'32.733"E	15°35'33.672"N	0.3658	32.8332	0.2098	33.5981
5	73°44'21.775"E	15°35'8.538"N	0.2391	32.1201	0.1823	34.0377

Figure 8 & table 3

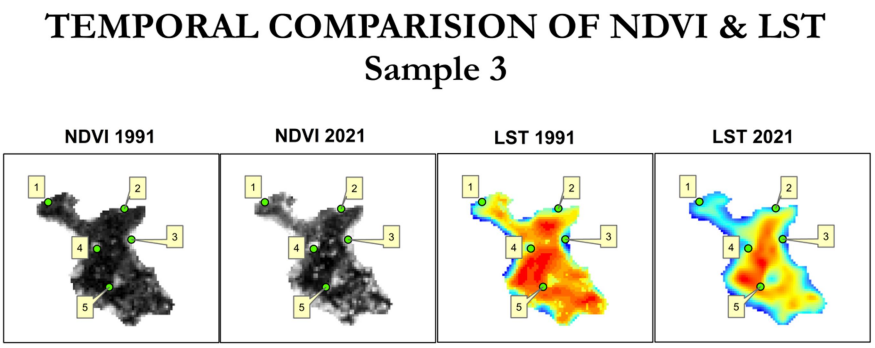

Sr.No.	Longitude	Latittude	NDVI_1991	LST_1991	NDVI_2021	LST_2021
1	73°49'58.143"E	15°34'33.09"N	0.2173	27.6272	0.199	32.4909
2	73°50'32.089"E	15°34'30.452"N	0.3442	27.1432	0.2716	32.365
3	73°50'35.276"E	15°34'17.168"N	0.4545	27.8288	0.2679	32.751
4	73°50'19.988"E	15°34'13.111"N	0.3589	29.6061	0.2318	35.085
5	73°50'25.504"E	15°33'56.644"N	0.175	32.5538	0.1332	36.9148

Figure 9 & Table 4

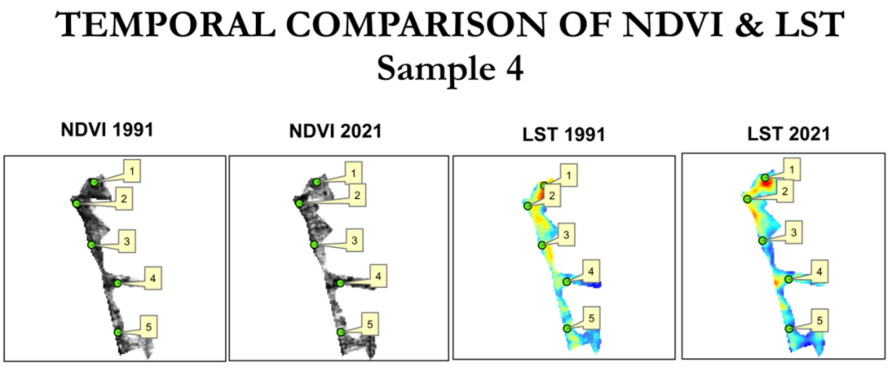

Sr.No.	Longitude	Latittude	NDVI_1991	LST_1991	NDVI_2021	LST_2021
1	73°45'11.583"E	15°33'55.474"N	0.247	31.715	0.2074	33.144
2	73°44'58.743"E	15°33'40.18"N	0.1494	30.0851	0.0841	33.7621
3	73°45'9.958"E	15°33'10.802"N	0.1914	29.2522	0.1373	33.135
4	73°45'29.355"E	15°32'43.434"N	0.2592	27.202	0.1038	32.8644
5	73°45'29.849"E	15°32'8.31"N	0.2631	28.03	0.2025	32.477

Figure 10 & Table 5

Interpretation

Four sites were chosen to depict extreme variation in NDVI and LST values. These four sites are most affected by de-vegetation which resulted in a change in land surface temperature. From sample 1, fig. 7 and table 2 for observation of 73°50’53.386” E and 15°37’38.768” N NDVI value has decreased from 0.21 to 0.16, and LST value increased from 30.9131 to 35.2322. NDVI value of 0.21 is considered as land under vegetation whereas 0.16 is considered as barren land. Such

observations can be made from the above samples and their corresponding tables. A general outlook can be drawn that de-vegetation results in a rise in land surface temperature.

CONCLUSION

- Vegetation cover is important for microscopic environmental change. The area which is lacking vegetation cover witnesses relatively higher land surface temperature. De-vegetation can be assessed through a comparison of NDVI values (**fig 3**).
- The land surface temperature in the study taluka (**fig. 4**) has changed dramatically over the last three decades.
- The highest temperature observed in 1991 was 38.1507 °C, while the lowest being 20.6068 °C whereas, for the year 2021, the maximum temperature observed is 40.5029 °C and the minimum is 27.3012 °C. A shift of 2.35 °C at the higher end and 6.69 °C at the lower end can be seen.
- This can be due to de-vegetation over time as a result of the increase in tourism, commercialization, urbanization, and industrialization.

REFERENCES

[1] F. Wang, Z. Qin, C. Song, L. Tu, A. Karnieli, and S. Zhao, "An improved mono-window algorithm for land surface temperature retrieval from Landsat 8 thermal infrared sensor data," *Remote Sens.*, vol. 7, no. 4, pp. 4268–4289, 2015, doi: 10.3390/rs70404268.

[2] J. Cristóbal, M. Ninyerola, and X. Pons, "Modeling air temperature through a combination of remote sensing and GIS data," *J. Geophys. Res. Atmos.*, vol. 113, no. 13, pp. 1–13, 2008, doi: 10.1029/2007JD009318.

[3] S. Guha, H. Govil, A. Dey, and N. Gill, "Analytical study of land surface temperature with NDVI and NDBI using Landsat 8 OLI and TIRS data in Florence and Naples city, Italy," *Eur. J. Remote Sens.*, vol. 51, no. 1, pp. 667–678, 2018, doi: 10.1080/22797254.2018.1474494.

[4] A. Bendib, H. Dridi, and M. I. Kalla, "Contribution of Landsat 8 data for the estimation of land surface temperature in Batna city, Eastern Algeria," *Geocarto Int.*, vol. 32, no. 5, pp. 503–513, 2017, doi: 10.1080/10106049.2016.1156167.

[5] Z. Qin, A. Karnieli, and P. Berliner, "A mono-window algorithm for retrieving land surface temperature from Landsat TM data and its application to the

Israel-Egypt border region," *Int. J. Remote Sens.*, vol. 22, no. 18, pp. 3719–3746, 2001, doi: 10.1080/01431160010006971.

[6] O. Rozenstein, Z. Qin, Y. Derimian, and A. Karnieli, "Derivation of land surface temperature for landsat-8 TIRS using a split window algorithm," *Sensors (Switzerland)*, vol. 14, no. 4, pp. 5768–5780, 2014, doi: 10.3390/s140405768.

[7] X. L. Chen, H. M. Zhao, P. X. Li, and Z. Y. Yin, "Remote sensing image-based analysis of the relationship between urban heat island and land use/cover changes," *Remote Sens. Environ.*, vol. 104, no. 2, pp. 133–146, 2006, doi: 10.1016/j.rse.2005.11.016.

[8] Y. Deng *et al.*, "Relationship among land surface temperature and LUCC, NDVI in typical karst area," *Sci. Rep.*, vol. 8, no. 1, pp. 1–12, 2018, doi: 10.1038/s41598-017-19088-x.

[9] Y. Tian, S. Wang, X. Bai, G. Luo, and Y. Xu, "Trade-offs among ecosystem services in a typical Karst watershed, SW China," *Sci. Total Environ.*, vol. 566–567, pp. 1297–1308, 2016, doi: 10.1016/j.scitotenv.2016.05.190.

[10] A. K. Bhandari, A. Kumar, and G. K. Singh, "Feature Extraction using Normalized Difference Vegetation Index (NDVI): A Case Study of Jabalpur City," *Procedia Technol.*, vol. 6, pp. 612–621, 2012, doi: 10.1016/j.protcy.2012.10.074.

[11] C. Ricotta, G. Avena, and A. De Palma, "Mapping and monitoring net primary productivity with AVHRR NDVI time-series: Statistical equivalence of cumulative vegetation indices," *ISPRS J. Photogramm. Remote Sens.*, vol. 54, no. 5–6, pp. 325–331, 1999, doi: 10.1016/S0924-2716(99)00028-3.

[12] X. Zhang, Y. Hu, D. Zhuang, Y. Qi, and X. Ma, "NDVI spatial pattern and its differentiation on the Mongolian Plateau," *J. Geogr. Sci.*, vol. 19, no. 4, pp. 403–415, 2009, doi: 10.1007/s11442-009-0403-7.

[13] V. Ihlen and K. Zanter, "Landsat 7 (L7) Data Users Handbook," *USGS Landsat User Serv.*, vol. 7, no. November, p. 151, 2019.

[14] U.S. Geological Survey, "Landsat 8 Data Users Handbook," *Nasa*, vol. 8, no. June, p. 97, 2016, [Online]. Available: https://landsat.usgs.gov/documents/Landsat8DataUsersHandbook.pdf.

[15] U. Avdan and G. Jovanovska, "Algorithm for automated mapping of land surface temperature using

LANDSAT 8 satellite data," *J. Sensors*, vol. 2016, 2016, doi: 10.1155/2016/1480307.

[16] H. Q. Xu and B. Q. Chen, "Remote sensing of the urban heat island and its changes in Xiamen City of SE China," *J. Environ. Sci.*, vol. 16, no. 2, pp. 276–281, 2004.

[17] Q. Weng, D. Lu, and J. Schubring, "Estimation of land surface temperature-vegetation abundance relationship for urban heat island studies," *Remote Sens. Environ.*, vol. 89, no. 4, pp. 467–483, 2004, doi: 10.1016/j.rse.2003.11.005.

[18] G. M. Gandhi, S. Parthiban, N. Thummalu, and A. Christy, "Ndvi: Vegetation Change Detection Using Remote Sensing and Gis - A Case Study of Vellore District," *Procedia Comput. Sci.*, vol. 57, pp. 1199–1210, 2015, doi: 10.1016/j.procs.2015.07.415.

[19] L. M. Montandon and E. E. Small, "The impact of soil reflectance on the quantification of the green vegetation fraction from NDVI," *Remote Sens. Environ.*, vol. 112, no. 4, pp. 1835–1845, 2008, doi: 10.1016/j.rse.2007.09.007.

[20] J. A. Sobrino *et al.*, "Land surface emissivity retrieval from different VNIR and TIR sensors," *IEEE Trans. Geosci. Remote Sens.*, vol. 46, no. 2, pp. 316–327, 2008, doi: 10.1109/TGRS.2007.904834.

[21] J. C. Jiménez-Muñoz, J. A. Sobrino, A. Plaza, L. Guanter, J. Moreno, and P. Martínez, "Comparison between fractional vegetation cover retrievals from vegetation indices and spectral mixture analysis: Case study of PROBA/CHRIS data over an agricultural area," *Sensors*, vol. 9, no. 2, pp. 768–793, 2009, doi: 10.3390/s90200768.

[22] N. H. Abu-Hamdeh, "Thermal properties of soils as affected by density and water content," *Biosyst. Eng.*, vol. 86, no. 1, pp. 97–102, 2003, doi: 10.1016/S1537-5110(03)00112-0.

[23] C.M. Thakar, S.S. Parkhe, A. Jain etal., 3d Printing: Basic principles and applications, Materials Today: Proceedings, https://doi.org/10.1016/j.matpr.2021.06.272

[24] Khan, R. M. I., Kumar, T., Supriyatno, T., &Nukapangu, V. (2021). The Phenomenon of Arabic-English Translation of Foreign Language Classes During The Pandemic. IjazArabi Journal of Arabic Learning, 4(3).

https://doi.org/10.18860/ijazarabi.v4i3.13597

[25] Sajja, G., Mustafa, M., Phasinam, K.,Kaliyaperumal, K., Ventayen, R., & Kassanuk, T. (2021). Towards Application of Machine Learning in Classification and Prediction of Heart Disease. 2021 Second International Conference On Electronics And Sustainable Communication Systems (ICESC).https://doi.org/10.1109/icesc51422.2021.9532940

[26] Veluri, R., Patra, I., Naved, M., Prasad, V.,Arcinas, M., Beram, S., & Raghuvanshi, A. (2021). Learning analytics using deep learning techniques for efficiently managing educational institutes. Materials Today:Proceedings. https://doi.org/10.1016/j.matpr.2021.11.416

[27] M. Stathopoulou and C. Cartalis, "Daytime urban heat islands from Landsat ETM+ and Corine land cover data: An application to major cities in Greece," *Sol. Energy*, vol. 81, no. 3, pp. 358–368, 2007, doi: 10.1016/j.solener.2006.06.014.